Tracking and Regulation Control of a Skid Steering Vehicle[*]

D. Pazderski,[1] K. Kozlowski,[1] and W. E. Dixon[2]

[1]Pozan University of Technology, Institute of Control and Systems Engineering, 60-965 Pozan, Poland
[2]Eng. Science and Technology Division-Robotics, Oak Ridge National Laboratory,
P.O. Box 2008, Oak Ridge, TN 37831-6305

Keywords: Skid Steering, Mobile Robot, and Robust Control

E-mail: dixonwe@ornl.gov, Telephone: (865)574-9025

Tracking and Regulation Control of a Skid Steering Vehicle

D. Pazderski[†], K. Kozlowski[†], and W. E. Dixon[‡]

[†]Poznan University of Technology, Institute of Control and Systems Eng., 60-965 Poznan, POLAND
[‡]Oak Ridge National Laboratory, 1 Bethel Valley Rd, P.O. Box 2008, Oak Ridge, TN 37831-6305, USA
email: pazderski@poczta.onet.pl, kk@ar-kari.put.poznan.pl, dixonwe@ornl.gov

Abstract - *Differentially driven skid-steering vehicles are often considered for navigation in outdoor terrains. However, the control of such vehicles is challenging because the wheels must skid laterally to follow a curved path, and motion stability can be lost as a result of excess skidding due to the position of the instantaneous center of rotation (ICR). To accommodate for the potential loss of stability due to the ICR, the development in this paper places an artificial operational nonholonomic constraint on the vehicle motion. Based on the operational constraint, a robust nonlinear controller is presented that can be used to achieve unified tracking and regulation of the vehicle. The dynamic model of the vehicle is also considered to incorporate further robustness to disturbances such as unknown vehicle properties and ground interaction forces.*

I. Introduction

Skid-steering mobile robots (SSMR) (e.g., the ATRV line of vehicles by iRobot, the PIONEER 3-AT by ActivMedia Robotics) are considered as all-terrain vehicles because of the robust nature of the mechanical structure. The robust mechanical nature of the robot is due, in part, to the lack of a steering system. Steering of a SSMR is achieved by differentially driving wheel pairs on each side of the robot. Although the steering scheme yields some mechanical benefits, the control of SSMR is challenging because the wheels must skid laterally to follow a curved path (i.e., the wheels are not aligned with the tangent of the path curve). If the projection of the instantaneous center of rotation (ICR) of the vehicle along the longitudinal axis becomes large the vehicle can loose motion stability as a result of excess skidding. In contrast, the ICR of traditional car-like vehicles is theoretically fixed along the rear wheel axis and the front wheels are steered tangent to the curved path. [1]

Although significant research has been directed at path planning and motion control for nonholonomic vehicles (see Dixon et al. [2], [3] for a review of the state of the art in mobile robot control), research that examines and accommodates for skid steering effects is sparse. Recently, Caracciolo et al. investigated the motion stability of the SSMR when the ICR moves out of the wheelbase. [4] Specifically, Caracciolo et al. imposed an artificial operational constraint on the vehicle that limited the projection of the ICR along the longitudinal axis to be confined to the wheelbase. A linearizing feedback kinematic controller was then developed to yield an exponential tracking result. Due to restrictions on the controller imposed by Brockett's condition, [5] the regulation problem is not solved. [4] To accommo-

date for the dynamics of a SSMR, a dynamic feedback linearizing controller was proposed that required exact model knowledge of the vehicle dynamics including the ground-wheel interaction forces. [4] To develop a more practical controller, a robust tracking controller was also proposed; however, the controller was only analyzed for straight line motion. [4]

Inspired by Caracciolo et al., an operational constraint is incorporated in the control design in this paper. In contrast to the research by Carraciolo et al., a kinematic control structure based on our previous research is exploited that simultaneously solves the tracking and regulation problems. [2] Specifically, the kinematic controller is based on the strategy of forcing some transformed states to track an exogenous exponentially decaying signal. This strategy yields a global exponential result for the transformed states and a global uniformly ultimately bounded (GUUB) result for the actual position and orientation tracking or regulation errors (i.e., the errors are bounded by an exponential envelope that reaches an arbitrarily small neighborhood about the origin). Motivated by practical issues such as the desire to accommodate for unknown ground interaction forces, a robust controller is developed that incorporates the uncertain dynamic model of the SSMR.

II. Kinematic Model

In this section, the kinematic model of the vehicle is developed. To develop the kinematic model, the kinematics of the free-body vehicle are developed along with the wheel kinematics. The wheel velocities are then related to the vehicle velocities to determine the complete vehicle kinematics.

A. Free-Body Kinematics
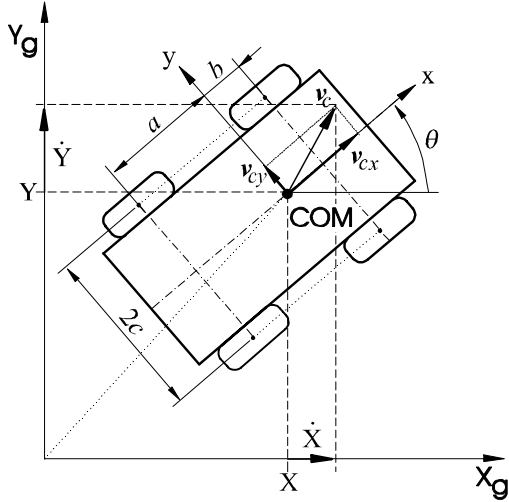
Fig. 1. Free body diagram.

To develop the kinematic model for a SSMR that is assumed to move in a plane (for simplicity) with an inertial coordinate system, denoted by (X_g, Y_g), and a local coordinate system, denoted by (x_l, y_l), where the origin of (x_l, y_l) is fixed to the center of mass (COM) of the SSMR as illustrated in Fig. 1. The position and orientation of the COM, denoted by $q(t) \in \mathbb{R}^3$, is defined as follows

$$ q \triangleq \begin{bmatrix} X & Y & \theta \end{bmatrix}^T \qquad (1) $$

where $X(t), Y(t) \in \mathbb{R}$ denote the position of the COM along the X_g and Y_g axes, and $\theta(t)$ denotes the counter-clockwise rotation of the the coordinate system (x_l, y_l) with respect to (X_g, Y_g). The linear velocity is defined as $v_c(t) \triangleq [v_{cx}(t), v_{cy}(t)]^T$ where $v_{cx}(t), v_{cy}(t) \in \mathbb{R}$ denote velocity components of the COM along the x_l and y_l axes, respectively, and $\omega_c(t) \triangleq \dot{\theta}(t)$ denotes the angular velocity. The following relationship can be developed from Fig. 1

$$ \begin{bmatrix} \dot{X} & \dot{Y} \end{bmatrix}^T = \begin{bmatrix} \cos\theta & -\sin\theta \\ \sin\theta & \cos\theta \end{bmatrix} v_c. \qquad (2) $$

B. Wheel Kinematics

To further develop the kinematic model of the SSMR, the ith wheel is considered as rotating with angular velocity $\omega_i(t)$, where $\omega_i(t) \in \mathbb{R} \; \forall i = 1, 2, \ldots, 4$ denotes the angular velocity control input for each wheel. For simplicity, the thickness of the wheel is neglected and is assumed to touch the plane at P_i as illustrated in Fig. 2. For traditional mobile robots, the wheel rotation is translated into a linear motion along the tangent of a curve without longitudinal slippage as described by the following expressions [6]

$$ v_{ix} = \omega_i r \qquad (3) $$
$$ v_{iy} = 0 \qquad (4) $$

where $r \in \mathbb{R}$ is the wheel radius. The relationship in (4) is only valid for a SSMR moving in a straight line. Since the wheels of a SSMR are not aligned with the curve tangent, $v_{iy}(t) \neq 0$ when $\omega_c(t) \neq 0$.

C. Wheels to Vehicle Relationships

The vectors $d_i(t) \triangleq [d_{ix}(t), d_{iy}(t)]^T$ and $d_C(t) \triangleq [d_{Cx}(t), d_{Cy}(t)]^T \in \mathbb{R}^2$ are expressed in (x_l, y_l) and are defined from the ICR of the vehicle to $P_i \; \forall i = 1, 2, \ldots, 4$ and from the ICR to the vehicle COM, respectively, as illustrated in Fig. 3. Based on the geometry of Fig. 3, the following expressions can be developed

$$ \frac{v_{ix}}{d_{iy}} = \frac{v_{cx}}{y_{ICR}} = \frac{v_{iy}}{d_{ix}} = -\frac{v_{cy}}{x_{ICR}} = \omega_c \qquad (5) $$

where we utilized the fact that the coordinates of the ICR expressed in (x_l, y_l), denoted by $x_{ICR}(t)$ and $y_{ICR}(t) \in \mathbb{R}$, are defined as follows

$$ \begin{bmatrix} x_{ICR} & y_{ICR} \end{bmatrix}^T = \begin{bmatrix} -d_{Cx} & d_{Cy} \end{bmatrix}^T. \qquad (6) $$

From Fig. 3, it is clear that the vectors $d_i(t)$ introduced in (5) satisfy the following relationships

$$ \begin{aligned} d_{1y} &= d_{2y} = d_{Cy} - c \\ d_{3y} &= d_{4y} = d_{Cy} + c \\ d_{1x} &= d_{4x} = d_{Cx} - a \\ d_{2x} &= d_{3x} = d_{Cx} + b \end{aligned} \qquad (7) $$

where $a, b, c \in \mathbb{R}$ are vehicle constants introduced in Fig. 1. Based on the development in (3) and (5)-(7), the individual angular wheel velocities (i.e., the kinematic control inputs) can be related to the individual longitudinal wheel velocities expressed in (x_l, y_l) as follows

$$ \begin{bmatrix} \omega_L = \omega_1 = \omega_2 \\ \omega_R = \omega_3 = \omega_4 \end{bmatrix} = \frac{1}{r} \begin{bmatrix} v_{1x} = v_{2x} \\ v_{3x} = v_{4x} \end{bmatrix} \qquad (8) $$

where $\omega_L(t), \omega_R(t) \in \mathbb{R}$ denote the angular velocities of the wheels on the left and right side of the vehicle, respectively, and r is given in (3). From (5)-(8), the following relationships can be developed to relate $\omega_L(t)$, $\omega_R(t)$ to the velocity of the COM expressed in (x_l, y_l)

$$ \begin{bmatrix} \omega_L \\ \omega_R \end{bmatrix} = \begin{bmatrix} \omega_c(d_{Cy} - c) \\ \omega_c(d_{Cy} + c) \end{bmatrix} = \begin{bmatrix} 1 & \frac{c}{x_{ICR}} \\ 1 & -\frac{c}{x_{ICR}} \end{bmatrix} \begin{bmatrix} v_{cx} \\ v_{cy} \end{bmatrix}. \qquad (9) $$

After simple algebraic manipulation, (9) can be used to develop the following measurable relationship between the wheel velocities and the velocity of the COM expressed in (x_l, y_l)

$$ \begin{bmatrix} \frac{\omega_L + \omega_R}{2} \\ \frac{\omega_L - \omega_R}{2} \end{bmatrix} = \begin{bmatrix} v_{cx} \\ v_{cy} \end{bmatrix}. \qquad (10) $$

Therefore, $v_c(t)$ is used in the subsequent development as the kinematic input.

Remark 1: The expressions in (5)-(7) can be used to determine that

$$\begin{bmatrix} v_{1y} = v_{4y} \\ v_{2y} = v_{3y} \end{bmatrix} = \begin{bmatrix} \omega_c(d_{Cx} - a) \\ \omega_c(d_{Cx} + b) \end{bmatrix} \tag{11}$$

$$= \begin{bmatrix} 0 & \frac{a}{x_{ICR}} \\ 0 & -\frac{b}{x_{ICR}} \end{bmatrix} \begin{bmatrix} v_{cx} \\ v_{cy} \end{bmatrix}.$$

From (11), it is clear that there is no possibility to control the lateral velocity of the wheels without knowledge of $x_{ICR}(t)$, the x_l-axis projection of the ICR.

D. Vehicle Kinematics

The following velocity constraint can be obtained from (5)

$$v_{cy} + x_{ICR}\dot{\theta} = 0. \tag{12}$$

After using (2) and (12) the following expression can be developed

$$\begin{bmatrix} -\sin\theta & \cos\theta & x_{ICR} \end{bmatrix} \begin{bmatrix} \dot{X} \\ \dot{Y} \\ \dot{\theta} \end{bmatrix} = A(q,t)\,\dot{q} = 0. \tag{13}$$

Since the generalized velocity $\dot{q}(t)$ is always in the null space of $A(q,t)$, it is possible to obtain the following kinematic relationship

$$\dot{q} = S(q,t)\,v_c, \tag{14}$$

where

$$S^T(q,t)\,A^T(q,t) = 0_{2\times 1} \tag{15}$$

and

$$S(q,t) \triangleq \begin{bmatrix} \cos\theta & -\sin\theta \\ \sin\theta & \cos\theta \\ 0 & -\frac{1}{x_{ICR}} \end{bmatrix}. \tag{16}$$

III. Dynamic Model

Researchers typically focus on the design of kinematic controllers and path planners to account for the nonholonomic motion constraints, with relatively few controllers that account for the dynamics of the vehicle. [2], [3], [7], [8] For SSMR, dynamic issues are especially important due to the unknown lateral skidding ground interaction forces. In this section, the wheel forces are examined, and the dynamic model of the vehicle is developed.

A. Wheel Dynamic Model

In Fig. 4, $F_i(t), N_i \in \mathbb{R}$ denote action forces related to the wheel torque and gravity respectively, and $F_{li}(\dot{q})$, $F_{si}(\dot{q}) \in \mathbb{R}$ denote lateral and longitudinal reaction forces due to friction. Assuming that there is no longitudinal slippage between wheel and surface, $F_i(t)$ is linearly dependent on the wheel torque control input, denoted by $\tau_i(t) \in \mathbb{R}$, as follows

$$F_i = r\tau_i. \tag{17}$$
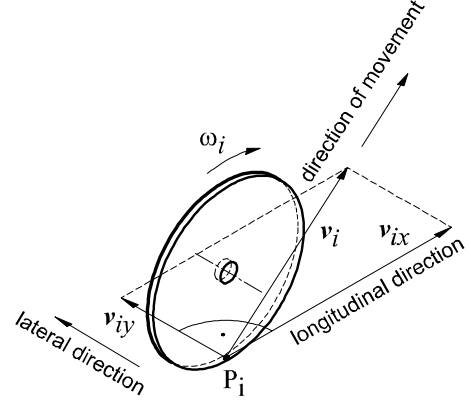
Fig. 2. Velocities of one drive wheel.
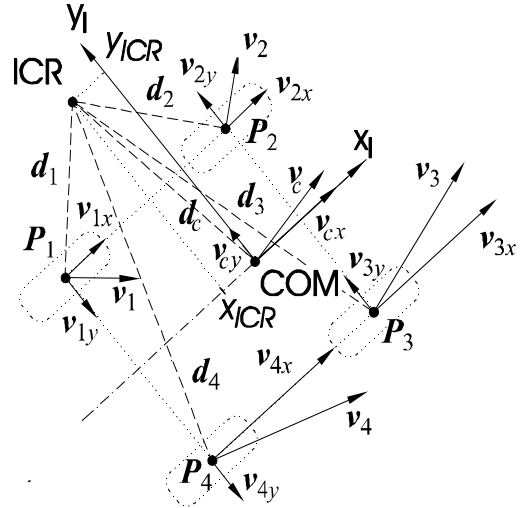
Fig. 3. Wheel and vehicle velocity relationships.
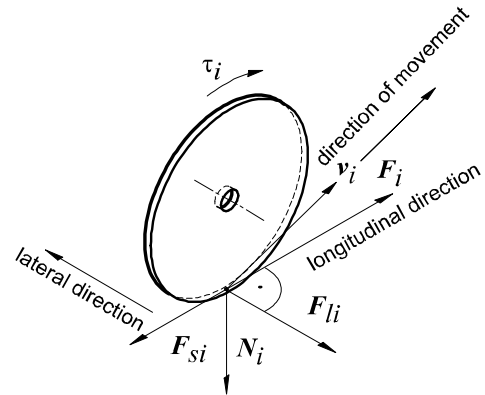
Fig. 4. Forces for one drive wheel.

Assuming symmetry about the longitudinal midline axis, N_i can be determined as follows

$$N_1 = N_4 = \frac{1}{2}\frac{b}{a+b}mg, \tag{18}$$

$$N_2 = N_3 = \frac{1}{2}\frac{a}{a+b}mg. \tag{19}$$

where g denotes gravity acceleration, a and b are depicted in Fig. 1, and m denotes the vehicle mass. The lateral and longitudinal reaction forces due to friction can be determined as follows

$$F_{li}(\dot{q}) = \mu_l N_i sgn(v_{yi}) \qquad F_{si}(\dot{q}) = \mu_s N_i sgn(v_{xi}) \tag{20}$$

where viscous friction effects have been neglected for simplicity. In (20), $sgn(\cdot)$ denotes the standard signum function, and μ_l, μ_s denote the static friction coefficients in the lateral and longitudinal direction, respectively, that are assumed to be equal for each wheel for simplicity.

B. Vehicle Dynamic Model

The dynamic model of the 4-wheel differentially driven, SSMR depicted in Fig. 1 can be expressed in the generalized coordinates as follows

$$M\ddot{q} + F = B\tau + A^T\lambda, \tag{21}$$

where $M \in \mathbb{R}^{3\times3}$ is a constant, diagonal, positive definite matrix, $F(q,\dot{q}) \in \mathbb{R}^3$ denotes the friction effects, $B(q) \in \mathbb{R}^{3\times2}$ denotes a torque transmission matrix, λ is a vector of constraint forces, and $\tau(t) \triangleq [\tau_r(t), \tau_l(t)]^T \in \mathbb{R}^2$ denotes a vector of torques produced by the angular velocities of the left and right wheels (see (8)), respectively. [2] The matrices M, $B(q)$, and $F(q,\dot{q})$ are defined as follows

$$M \triangleq \begin{bmatrix} m & 0 & 0 \\ 0 & m & 0 \\ 0 & 0 & I \end{bmatrix} \quad B(q) \triangleq \frac{1}{r}\begin{bmatrix} \cos\theta & \cos\theta \\ \sin\theta & \sin\theta \\ -c & c \end{bmatrix}$$

$$F(q,\dot{q}) \triangleq \begin{bmatrix} F_s(\dot{q})\cos\theta - F_l(\dot{q})\sin\theta \\ F_s(\dot{q})\sin\theta + F_l(\dot{q})\cos\theta \\ M_r(\dot{q}) \end{bmatrix} \tag{22}$$

where $I \in \mathbb{R}$ denotes the moment of inertia about the COM, c is depicted in Fig. 1, $F_s(\dot{q}) \in \mathbb{R}$ is a resultant longitudinal resistance force, $F_l(\dot{q}) \in \mathbb{R}$ is a resultant lateral force, and $M_r(\dot{q}) \in \mathbb{R}$ denotes a resistive moment around the center of mass. [4] In (22), $F_s(\dot{q})$ and $F_l(\dot{q})$ are defined as follows

$$F_s(\dot{q}) \triangleq \sum_{i=1}^4 F_{si}(\dot{q}), \quad F_l(\dot{q}) \triangleq \sum_{i=1}^4 F_{li}(\dot{q}),$$

and the resistive moment is defined as

$$M_r(\dot{q}) \triangleq b(F_{l2}(\dot{q}) + F_{l3}(\dot{q})) - a(F_{l1}(\dot{q}) + F_{l4}(\dot{q})) + c(-F_{s1}(\dot{q}) - F_{s2}(\dot{q}) + F_{s3}(\dot{q}) + F_{s4}(\dot{q}))$$

where $F_{si}(\dot{q})$ and $F_{li}(\dot{q})$ are defined in (20). [4]

IV. Control Development

A. Operational Constraint

For straight line motion, the coordinates of the ICR expressed in (x_l, y_l) are $(0, \infty)$; hence, (12) can be used to conclude that $v_{cy}(t) = 0$ (i.e., there is no lateral skidding). For curved motion, the x_l-axis projection of the ICR becomes nonzero, and (12) indicates that $v_{cy}(t) \neq 0$ (i.e., lateral skidding occurs). Some lateral skidding is required to enable the vehicle to traverse curved paths; however, excessive skidding can result in a loss of motion stability. Carraciolo et al. quantify excessive skidding as the value of $v_{cy}(t)$ when $|x_{ICR}(t)|$ is greater than the wheelbase (e.g., if $|x_{ICR}(t)| > a$). [4]

To develop a controller that limits the magnitude of the skidding, a so-called operational nonholonomic constraint on the vehicle motion can be incorporated. [4] Specifically, the following constraint is artificially imposed on the motion of the vehicle from (12)

$$v_{cy} + x_0\dot{\theta} = 0 \tag{23}$$

where $x_0 \in \mathbb{R}$ is a positive constant (i.e., a skid limiting gain). For example, x_0 could be selected as $0 < x_0 < a$ to ensure that $|x_{ICR}(t)| > a$. [4] By introducing the artificial constraint in (23), the expression in (16) can be rewritten as follows

$$S(q) \triangleq \begin{bmatrix} \cos\theta & -\sin\theta \\ \sin\theta & \cos\theta \\ 0 & -\frac{1}{x_0} \end{bmatrix}. \tag{24}$$

B. Tracking Control Objective

The control objective for the robot is to ensure that $q(t)$ tracks a reference position and orientation, denoted by $q_r(t) \triangleq [X_r(t), Y_r(t), \theta_r(t)]^T \in \mathbb{R}^3$. To quantify this objective, a pose tracking error, denoted by $\tilde{q}(t) \in \mathbb{R}^3$, is defined as follows

$$\tilde{q} \triangleq q - q_r = \begin{bmatrix} \tilde{X} & \tilde{Y} & \tilde{\theta} \end{bmatrix}^T. \tag{25}$$

The SSMR reference trajectory can be generated as follows

$$\dot{q}_r = S(q_r)v_r \tag{26}$$

where $S(\cdot)$ was defined in (24), and $v_r(t) \triangleq [v_{cxr}(t), v_{cyr}(t)]^T \in \mathbb{R}^2$ denotes the reference velocity. [9], [10] With regard to (26), it is assumed that the signal $v_r(t)$ is constructed to produce the desired motion and that $v_r(t)$, $\dot{v}_r(t)$, $q_r(t)$, and $\dot{q}_r(t)$ are bounded for all time.

C. Kinematic Control

C.1 Transformation

To facilitate the development of the kinematic controller, the auxiliary variables $w(t) \in \mathbb{R}$ and $z(t) \in \mathbb{R}^2$ are related to the tracking errors introduced in (25) as follows [2]

$$\begin{bmatrix} w & z^T \end{bmatrix}^T \triangleq P\left(\theta, \tilde{\theta}\right)\tilde{q}. \tag{27}$$

In (27), the global invertible transformation $P\left(\theta, \tilde{\theta}\right) \in \mathbb{R}^{3\times 3}$ is defined as [2]

$$P\left(\theta, \tilde{\theta}\right) \triangleq \begin{bmatrix} p_{11} & p_{12} & -2x_0 \\ 0 & 0 & 1 \\ \cos\theta & \sin\theta & 0 \end{bmatrix} \quad (28)$$

where $p_{11}\left(\theta, \tilde{\theta}\right), p_{12}\left(\theta, \tilde{\theta}\right) \in \mathbb{R}$ are defined as

$$p_{11}\left(\theta, \tilde{\theta}\right) \triangleq -\tilde{\theta}\cos\theta + 2\sin\theta$$
$$p_{12}\left(\theta, \tilde{\theta}\right) \triangleq -\tilde{\theta}\sin\theta - 2\cos\theta.$$

The structure of the transformation introduced in (27) is motivated from the resulting open-loop system. Specifically, after taking the time derivative of (27), an open-loop system is obtained that is similar to Brockett's non-holonomic integrator [5]

$$\dot{w} = u^T J^T z + f \quad (29)$$
$$\dot{z} = u.$$

In (29), $J \in \mathbb{R}^{2\times 2}$ denotes the following skew-symmetric matrix

$$J \triangleq \begin{bmatrix} 0 & -1 \\ 1 & 0 \end{bmatrix}, \quad (30)$$

the auxiliary kinematic control signal $u(t) \in \mathbb{R}^2$ is related to the kinematic control input $v_c(t)$ as follows

$$u = T^{-1}v_c - \begin{bmatrix} -\frac{v_{cyr}}{x_0} \\ v_{cxr}\cos z_1 + v_{cyr}\sin z_1 \end{bmatrix} \quad (31)$$

where $T(q, \tilde{q}) \in \mathbb{R}^{2\times 2}$ is defined as

$$T \triangleq \begin{bmatrix} L & 1 \\ -x_0 & 0 \end{bmatrix} \quad (32)$$

and $L(q, \tilde{q}) \triangleq \tilde{X}(t)\sin\theta - \tilde{Y}(t)\cos\theta$ is an auxiliary variable that has a distance meaning, and $f(t) \in \mathbb{R}$ is defined as

$$f \triangleq 2\left[-v_{cxr}\sin z_1 + v_{cyr}\left(\cos z_1 - \frac{z_2}{x_0} - 1\right)\right]. \quad (33)$$

The inverse relationship in (31) can be determined as follows

$$v_c = Tu + \Pi, \quad (34)$$

where

$$\Pi \triangleq \begin{bmatrix} v_{cxr}\cos z_1 + v_{cyr}\left(\sin z_1 - \frac{L}{x_0}\right) \\ v_{cyr} \end{bmatrix}. \quad (35)$$

Based on (10) and (31), $u(t)$ is considered as the kinematic control input in the subsequent sections.

C.2 Control Design

The focus of the previous development was to craft an open-loop error system that incorporated an artificial operational constraint to limit lateral skidding by the vehicle as in Carraciolo et al. [4] Now the aim is to design the kinematic controller. In contrast to the research in Carraciolo et al. [4] that restricts $v_{cx}(t) \neq 0$ (i.e., the regulation problem can not be solved), to achieve a unified tracking and regulation result the following kinematic control structure leverages on research by Dixon et al. [2]

$$u \triangleq u_a - k_2 z. \quad (36)$$

In (36), $u_a(t) \in \mathbb{R}^2$ is defined as

$$u_a \triangleq \left(\frac{k_1 w + f}{\delta_d^2}J + \Omega_1\right)z_d \quad (37)$$

where $k_1, k_2 \in \mathbb{R}$ denote positive constant design parameters. The kinematic control design is motivated by a strategy to force the transformed tracking error signal $z(t)$ to track an auxiliary desired signal $z_d(t) \in \mathbb{R}^2$ that is generated from the following differential equation

$$\dot{z}_d \triangleq \left[\frac{\dot{\delta}_d}{\delta_d} + \left(\frac{k_1 w + f}{\delta_d^2} + w\Omega_1\right)J\right]z_d \quad (38)$$

and initial condition

$$z_d^T(0)z_d(0) = \delta_d^2(0). \quad (39)$$

An auxiliary error signal, denoted by $\tilde{z}(t) \in \mathbb{R}^2$, is defined as follows to quantify the tracking performance

$$\tilde{z} \triangleq z_d - z. \quad (40)$$

The structure of (38) and the initial condition provided in (39) can be used to prove that [2]

$$\|z_d(t)\| = \delta_d^2(t)$$

where $\Omega_1(t), \delta_d(t) \in \mathbb{R}$ are auxiliary terms defined as follows

$$\Omega_1 \triangleq k_2 + \frac{\dot{\delta}_d}{\delta_d} + w\frac{k_1 w + f}{\delta_d^2} \quad (41)$$

$$\delta_d \triangleq \alpha_0 \exp(-\alpha_1 t) + \varepsilon_1 \quad (42)$$

and $\alpha_0, \alpha_1, \varepsilon_1 \in \mathbb{R}$ are positive constant design parameters. After substituting (36)-(42) into the open-loop error system in (29), the following closed-loop error system can be obtained [2]

$$\dot{w} = u_a^T J\tilde{z} - k_1 w \quad (43)$$

$$\dot{\tilde{z}} = -k_2\tilde{z} + wJu_a. \quad (44)$$

C.3 Stability Analysis

Based on the open-loop error system in (29) and the control structure in (36)-(42), the following theorem can be developed. [2]

Theorem 1: Provided the desired trajectory (i.e., $v_r(t)$, $\dot{v}_r(t)$, $q_r(t)$, and $\dot{q}_r(t)$) is selected to be bounded for all time $t \geq 0$, the kinematic controller given in (36)-(42) ensures the position and orientation tracking errors defined in (25) are GUUB in the sense that

$$\left|\tilde{X}(t)\right|, \left|\tilde{Y}(t)\right|, \left|\tilde{\theta}(t)\right| \leq \beta_0 \exp(-\gamma_0 t) + \beta_1 \varepsilon_1 \qquad (45)$$

where ε_1 was introduced in (42), and β_0, β_1, and $\gamma_0 \in \mathbb{R}$ are some positive constants.

Proof: Let $V(w(t), \tilde{z}(t)) \in \mathbb{R}$ denote the following non-negative function [2]

$$V = \frac{1}{2}w^2 + \frac{1}{2}\tilde{z}^T\tilde{z}. \qquad (46)$$

After taking the time derivative of (46) and making the appropriate substitutions from (43) and (44), the following inequality can be obtained

$$\dot{V} \leq -2\min(k_1, k_2)V. \qquad (47)$$

Standard arguments can now be employed to solve the differential inequality given in (47) to obtain the following inequalities [2]

$$\|\Psi_1(w(t), \tilde{z}(t))\| \leq \exp(-\min(k_1, k_2)t) \|\Psi_1(w(0), \tilde{z}(0))\| \qquad (48)$$

$$\begin{aligned}
\|z\| &\leq \|\tilde{z}\| + \|z_d\| \\
&\leq \exp(-\min(k_1, k_2)t) \|\Psi_1(w(0), \tilde{z}(0))\| \qquad (49) \\
&\quad + \alpha_0 \exp(-\alpha_1 t) + \varepsilon_1
\end{aligned}$$

where the vector $\Psi_1(w(t), \tilde{z}(t)) \in \mathbb{R}^3$ is defined as

$$\Psi_1 = \begin{bmatrix} w & \tilde{z}^T \end{bmatrix}^T. \qquad (50)$$

By using the results in (48) and (49) along with the inverse of the transformation introduced in (27) and (28), the result in (45) can be obtained. [2]

Remark 2: No restrictions are placed on the desired trajectory $v_r(t)$, $\dot{v}_r(t)$, $q_r(t)$, and $\dot{q}_r(t)$ that would not allow the vehicle to stop at a desired goal position. Hence, it is straightforward that the kinematic controller can also be used to solve the regulation problem.

D. Dynamic Control

Inclusion of the dynamic model in the control design is motivated by the desire to improve the robustness of the control design. One method to include the dynamic model is to feedback linearize the dynamic equations; however, this is impractical because of unknown lateral skidding forces associated with the SSMR. Therefore, it is essential to design a controller which is robust to the dynamic unmodeled disturbances. [11] To facilitate

the subsequent development and analysis, the dynamic model in (21) can be rewritten in terms of $u(t)$ as follows

$$\bar{M}\dot{u} + \bar{C}u + \bar{F} = \bar{B}\tau, \qquad (51)$$

where

$$\begin{aligned}
\bar{M} &= (ST)^T M (ST) \\
\bar{C} &= T^T \left(S^T M \dot{S}T + S^T M S\dot{T}\right) \\
\bar{F} &= T^T \left(S^T M \dot{S}\Pi + S^T M S\dot{\Pi} + S^T F\right) \\
\bar{B} &= (ST)^T B.
\end{aligned} \qquad (52)$$

From (22) and (52), it is clear that

$$\dot{\bar{M}} = \bar{C} + \bar{C}^T \qquad (53)$$

and that the following skew-symmetric relationship exists

$$\xi^T \left(\bar{C}^T - \bar{C}\right) \xi = 0 \qquad \forall \xi \in \mathbb{R}^2. \qquad (54)$$

Based on the fact that the kinematic controller in (36)-(42) is continuous, backstepping techniques can be used to incorporate the dynamic effects. [2], [12] Specifically, since the transformed velocity signal $u(t)$ is no longer a control input, a desired velocity signal, denoted by $u_d(t) \in \mathbb{R}^2$, is designed based on (36) as follows

$$u_d \triangleq u_a - k_2 z. \qquad (55)$$

The dynamic model in (51) can be expressed in terms of $u_d(t)$ and then linearly parameterized as follows

$$\bar{M}\dot{u}_d + \bar{C}u_d + \bar{F} = Y_d\theta, \qquad (56)$$

where $\theta \in \mathbb{R}^4$ is the following vector of unknown positive constants

$$\theta = \begin{bmatrix} m & I & \mu_s mg & \mu_l mg \end{bmatrix}^T \qquad (57)$$

and $Y_d\left(q_d, \dot{q}_d, q_r, \dot{q}_r, u_d, \dot{u}_d\right) \in \mathbb{R}^{2\times 4}$ is a known regression that is a function of the desired transformed velocity and acceleration. A constant, best-guess estimate for the unknown parameters in (57) is defined as $\theta_0 \in \mathbb{R}^4$. A parameter estimate error, denoted by $\tilde{\theta} \in \mathbb{R}^4$, is defined as follows

$$\tilde{\theta} = \theta_0 - \theta \qquad (58)$$

where the norm of $\tilde{\theta}$ can be upper bounded by a known positive constant $\rho \in \mathbb{R}$ as

$$\left\|\tilde{\theta}\right\| \leq \rho. \qquad (59)$$

The closed-loop error system for $w(t)$ and $\tilde{z}(t)$ can be determined as follows [2]

$$\begin{aligned}
\dot{w} &= -k_1 w + u_a^T J\tilde{z} + \tilde{u}^T Jz \qquad (60) \\
\dot{\tilde{z}} &= -k_2 \tilde{z} + wJu_a + \tilde{u} \qquad (61)
\end{aligned}$$

where $\tilde{u}(t) \in \mathbb{R}^2$ denotes the following backstepping error signal

$$\tilde{u} = u_d - u. \qquad (62)$$

To develop the torque control input, we consider a Lyapunov function candidate, denoted as $V_2(w, \tilde{z}, \tilde{u}) \in \mathbb{R}$, as follows

$$V_2(w, \tilde{z}, \tilde{u}) = \frac{1}{2}w^2 + \frac{1}{2}\tilde{z}^T\tilde{z} + \frac{1}{2}\tilde{u}^T\bar{M}\tilde{u}.$$

After taking the time derivative of $V_2(w, \tilde{z}, \tilde{u})$ and substituting for the closed-loop error systems in (60) and (61), the following expression can be obtained

$$
\begin{aligned}
\dot{V}_2(w, \tilde{z}, \tilde{u}) &= -k_1 w^2 - k_2\tilde{z}^T\tilde{z} + \tilde{u}^T(wJz + \tilde{z}) \quad (63)\\
&\quad + \tilde{u}^T\left(\bar{M}\dot{u}_d + \bar{C}u + \bar{F} - \bar{B}\tau + \frac{1}{2}\dot{\bar{M}}\tilde{u}\right)
\end{aligned}
$$

where (51) and (62) were utilized. The following expression can be obtained after utilizing (53) and (54), and then adding and subtracting the term $\tilde{u}^T(t)\bar{C}(\cdot)u_d(t)$ to the right side of (63)

$$
\begin{aligned}
\dot{V}_2(w, \tilde{z}, \tilde{u}) &= -k_1 w^2 - k_2\tilde{z}^T\tilde{z} + \tilde{u}^T(wJz + \tilde{z}) (64)\\
&\quad + \tilde{u}^T\left(\bar{M}\dot{u}_d + \bar{C}u_d + \bar{F} - \bar{B}\tau\right).
\end{aligned}
$$

After using (56), (64) can be rewritten as follows

$$\dot{V}_2(w, \tilde{z}, \tilde{u}) = -k_1 w^2 - k_2\tilde{z}^T\tilde{z} + \tilde{u}^T\left(wJz + \tilde{z} + Y_d\theta - \bar{B}\tau\right) \tag{65}$$

Based on (65), the torque control input is designed as follows

$$\tau = \bar{B}^{-1}\left(wJz + \tilde{z} + Y_d\theta_0 + \tau_a + k_3\tilde{u}\right) \tag{66}$$

where $\tau_a(t) \in \mathbb{R}^2$ denotes a robust control term designed as follows

$$\tau_a = Y_d\frac{\rho^2 Y_d^T\tilde{u}}{\|Y_d^T\tilde{u}\|\rho + \varepsilon_2}, \tag{67}$$

where $\varepsilon_2 \in \mathbb{R}$ is an adjustable positive constant. After substituting (66) and (67) into (65), the following expression is obtained

$$
\begin{aligned}
\dot{V}_2(w, \tilde{z}, \tilde{u}) &= -k_1 w^2 - k_2\tilde{z}^T\tilde{z} - k_3\tilde{u}^T\tilde{u} \quad (68)\\
&\quad + \left(Y_d^T\tilde{u}\right)^T\left(\tilde{\theta} - \frac{\rho^2 Y_d^T\tilde{u}}{\|Y_d^T\tilde{u}\|\rho + \varepsilon_2}\right).
\end{aligned}
$$

By utilizing the following inequality

$$0 \leq \frac{\|Y_d^T\tilde{u}\|\rho\varepsilon_2}{\|Y_d^T\tilde{u}\|\rho + \varepsilon_2} \leq \varepsilon_2, \tag{69}$$

the expression in (68) can be rewritten as follows

$$\dot{V}_2(w, \tilde{u}, \tilde{u}) \leq -k_1 w^2 - k_2\tilde{z}^T\tilde{z} - k_3\tilde{u}^T\tilde{u} + \varepsilon_2. \tag{70}$$

Based on (70), similar stability analysis techniques as outlined for the proof of Theorem 1, can be used to prove the following theorem.

Theorem 2: Provided the desired trajectory is selected so that $q_r(t), \dot{q}_r(t), v_r(t), \dot{v}_r(t) \in \mathcal{L}_\infty$, the robust controller given in (37), (38), (41), (42), (55), (66), and (67) ensures the position and orientation tracking errors are GUUB as follows

$$\|\tilde{q}\| \leq \sqrt{\beta_1\exp(-\gamma_1 t) + \varepsilon_2\beta_2} + \beta_3\exp(-\gamma_2 t) + \beta_{4\varepsilon 1},$$

where $\gamma_1, \gamma_2, \beta_1, \beta_2, \beta_3, \beta_4 > 0$. [2]

V. Conclusion

Regulation and tracking control of a 4 wheel differentially driven, skid-steering vehicle is considered in this paper. Inspired by the research in Carraciolo et al., an artificial nonholonomic operational constraint was incorporated in the control design to minimize lateral skidding. Specifically a skid limiting control parameter is incorporated that limits the longitudinal component of the projection of the ICR (e.g., to remain inside the wheelbase) on the local coordinate system attached to the vehicle. In contrast to the research in Carraciolo et al., both the tracking and regulation problems are solved with a robust controller that rejects disturbances due to dynamic properties of the vehicle including unknown ground interaction forces.

References

[1] J. P. LAUMOND (ed.), *Robot Motion Planning and Control*, LNCIS Volume 229, Springer-Verlag, London, (1998).

[2] W. E. DIXON, D. M. DAWSON, E. ZERGEROGLU, and A. BEHAL, *Nonlinear Control of Wheeled Mobile Robots*, LNCIS Volume 262, Springer-Verlag, London, (2001).

[3] W. E. DIXON, M. S. DE QUEIROZ, D. M. DAWSON, and T. J. FLYNN, "Adaptive Tracking and Regulation Control of a Wheeled Mobile Robot with Controller/Update Law Modularity," *IEEE Transactions on Control Systems Technology*, accepted, to appear; see also *Proceedings of the IEEE International Conference on Robotics and Automation*, p. 2620, Washington, DC, (2002).

[4] L. CARACCIOLO, A. DE LUCA, S. IANNITTI, "Trajectory Tracking Control of a Four-Wheel Differentially Driven Mobile Robot," *Proc. of the IEEE International Conference on Robotics and Automation*, p. 2632, Detroit, MI, (1999).

[5] R. W. BROCKETT, "Asymptotic Stability and Feedback Stabilization," *Differential Geometric Control Theory* edited by R. W. BROCKETT, R. S. MILMAN and H. J. SUSMANN, Birkhauser, Boston, p. 181, (1983).

[6] B. D'ANDREA-NOVEL, G. CAMPION, G. BASTIN, "Control of Nonholonomic Wheeled Mobile Robots by State Feedback Linearization," *The International Journal of Robotics Research*, (1995).

[7] W. DONG and W. HUO, "Adaptive Stabilization of Dynamic Nonholonomic Chained Systems with Uncertainty", *Proc. of the 36th IEEE Conference on Decision and Control*, p. 2362, (1997).

[8] R. McCLOSKEY and R. MURRAY, "Exponential Stabilization of Driftless Nonlinear Control Systems Using Homogeneous Feedback," *IEEE Transactions on Automatic Control*, **42**, 5, p. 614, (1997).

[9] Z. JIANG and H. NIJMEIJER, "Tracking Control of Mobile Robots: A Case Study in Backstepping," *Automatica*, **33**, 7, p. 1393, (1997).

[10] Y. KANAYAMA, Y. KIMURA, F. MIYAZAKI, and T. NOGUCHI, "A Stable Tracking Control Method for an Autonomous Mobile Robot," *Proc. of the IEEE International Conference on Robotics and Automation*, p. 384, (1990).

[11] K. KOZLOWSKI and D. PAZDERSKI, "Control of a Four-Wheel Vehicle Using Kinematic Oscillator," *Proc. of the Sixth International Conference on Climbing and Walking Robots and their Supporting Technologies*, p. 135, (2003).

[12] K. KOZLOWSKI and J. MAJCHRZAK, "A New Control Algorithm for a Nonholonomic Mobile Robot," *Archives of Control Sciences*, **12**, p. 37, (2002).